Bidirectional Gigabits Per Second Spatial Diversity Link Using POF for Passive Optical Front-Ends

Bidirectional Gigabits Per Second Spatial Diversity Link Using POF for Passive Optical Front-Ends

Carina Barbio, *Student Member, IEEE*, Ketemaw Addis Mekonnen, *Member, IEEE*, Frans Huijskens, Ton Koonen, *Fellow, IEEE*, and Eduward Tangdiongga, *Member, IEEE*

***Abstract*—This paper presents a novel concept for spatial diversity using plastic optical fibre (POF)-based luminaire transmission for in-home networks. We show the feasibility of an optical transmission system using POFs, acting as optical front-haul, for realizing a high capacity wireless bidirectional link aided by a spatial diversity scheme allowing user mobility around the access points. The light coming out of the 1 mm core diameter step-index POF is highly divergent and, therefore, for each POF-end an optical lens is placed to adjust the size of wireless cells, in order to allow user's mobility or to adjust the number of users served by the access points. Thus, the access points are completely passive, hence no electrical powering is needed, resulting in low maintenance. In addition, active components such as light sources and detectors can be located remotely from the access points and they are connected to each other by POFs. Futhermore, we performed optical wireless experiments with an eye-safe visible light laser and therefore our wireless link is limited to 1.2 m and 45 cm diameter of coverage areas. We obtained multi-Gbps for downlink and uplink and compared the link performance using discrete multitone, pulse amplitude modulation, and Nyquist sub-carrier modulation.**

***Index Terms*—Fronthaul, home networks, LiFi, plastic optical fibre, spatial diversity, visible light communication.**

I. Introduction

THE new features of the Internet of Things (IoT) are causing a large increase in the number of interconnected wireless devices, leading to a higher demand for wireless connections, specially in indoor environments. For the next generation of IoT, devices such as robots, cellphones, tablets, drones and others, will produce a large amount of high resolution and high accurate information, which will require even more bandwidth and capacity for the wireless systems. For these reasons, the radio frequency (RF) spectrum is becoming overcrowded, leading to a need to search for new spectrum opportunities. In addition, some applications have limitation in the use of Wi-Fi, where electromagnetic interference (EMI)-related safety is required, such as: in-flight communication/entertainment, petrochemicals plants, factory control rooms, etc. This gives rise for adopting optical wireless communication (OWC) technologies. OWC uses light waves as transmission media and works in the unlicensed optical spectrum, which offers large bandwidth [1]. The optical spectrum offers the use of visible (400–700 nm) and infrared telecom (1500–1600 nm) wavelengths range. The visible spectrum can offer 320 THz of bandwidth and the infrared can offer 12.5 THz. Both transmission spectra offer much larger bandwidth than provided by the RF spectrum [2]. Another main advantage of the OWC is that optical signals do not propagate through the walls, hence the communication is restricted inside the rooms, which increases security and avoids jamming from outside the room. Among the various OWC technologies, the visible light communication (VLC), a.k.a. Light Fidelity (LiFi), is one of the most promising and increasingly becoming commercially available. The main advantage of the LiFi system is that it piggybacks the existing lighting infrastructure, hence the components are widely available at low costs. Therefore, this LiFi technology is mostly suited for cost-sensitive network deployments such as home networks where no cost sharing can be implemented and home owners are fully responsible for costs regarding installation, maintenance and operation of their network. LiFi makes use of light emitting diodes (LEDs) for transmitters and silicium photodiodes (SiPD) for receivers.

Recent progress on LiFi transceivers shows in [3]–[5] that throughputs higher than 8 Gbps can be achieved using direct modulated RGB-type LEDs on a wireless VLC link, without considering the feeding network. Although being low cost, the existing LEDs are usually used for illumination, thus when used for data communication at higher speeds (gigabit range), they present high non-linearity and narrow modulation bandwidth, around 20 MHz. An alternative solution is to use smaller area LEDs, such as μLEDs, that can provide higher modulation bandwidth when used with higher current densities [6]. In [7] a transmission with a fabricated green color InGaN/GaN μLED, with 1.102 GHz 3-dB bandwidth and considering 0.25 m free space and achieving a throughput of 4.343 Gbps. However, the μLEDs suffer from efficiency droop when high current densities are applied, leading to a higher cost of the LEDs and undermining the reason to use them. Another solution is to use larger bandwidth laser diodes (LDs) at the ceiling. LDs provide better performance in terms of linearity, bandwidth and emitting power, when compared to LEDs. Although achieving high throughputs, the previously mentioned papers, do not make use of any feeder line. Thus, they do not approach one of the main

Manuscript received 28 February 2022; revised 21 July 2022; accepted 26 July 2022. Date of publication 28 July 2022; date of current version 21 October 2022. This work was supported by the European Union's Horizon 2020 Innovation Action Project Enhance Lighting for the Internet of Things (ELIoT) under Grant 825651. (*Corresponding author: Carina Barbio.*)

The authors are with the Electro-Optical Communication System Group at the Eindhoven University of Technology 5612AP Eindhoven, The Netherlands (e-mail: c.ribeiro.barbio.correa@tue.nl; k.a.mekonnen@tue.nl; f.m.huijskens@tue.nl; a.m.j.koonen@tue.nl; e.tangdiongga@tue.nl).

Color versions of one or more figures in this article are available at https://doi.org/10.1109/JLT.2022.3194649.

Digital Object Identifier 10.1109/JLT.2022.3194649

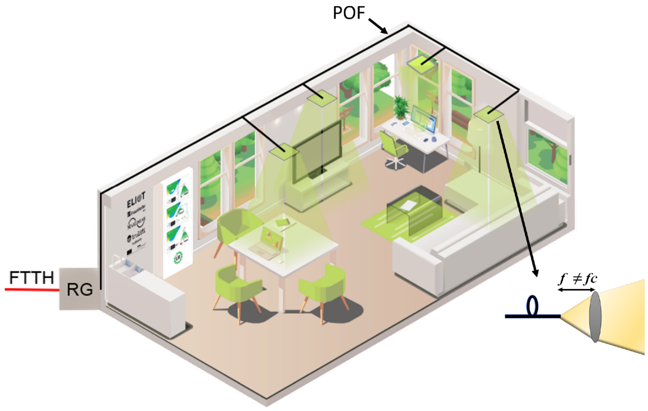

Fig. 1. In-home network employing POFs as transmission medium. POF-ends serve as passive optical front-ends, thus no optical-electrical-optical conversion, for transmitting and receiving light with a lens placed at a defocused position ($f \neq f_c$) to create coverage areas. RG - residential gateway. [Courtesy of KPN].

issues for in-home networks, how to bring high data rates from a residential gateway (RG) where fibre-to-the-home is terminated, to each room in a cost-effective way.

In [8] it was highlighted that one of the challenges of the LiFi systems is the optimization of data densities in a wireless cell. Currently the LiFi systems use powerline, coax, and Cat-5 as the feeder line for the ceiling luminaires. In [9] an architecture using POFs as an analog fronthaul technology integrated with LiFi luminaires is discussed and a throughput for downlink/uplink of 313 Mbps/218 Mbps, using 10 m POF and 70 cm between AP and user, is achieved. In our previous work [10] we proposed to use optical fibres, that would be remotely fed by a broadband LDs in the RG, as the feeder line to the room ceilings. The main advantage of the proposed system is that no electrical powering and zero maintenance would be needed for the ceiling infrastructure, bringing considerable installation and operational benefits in terms of overall costs. These advantages make this system a good suit for an in-home communication network, which relies, for cost reasons, heavily on its simplicity in providing high capacity to wireless users.

To support several services, a converged network, as presented in Fig 1, needs large bandwidth, small dimension, low losses, and EMI free. Several optical networks can be used to comply with these requirements and carry the data from the RG to each room. Silica single-mode and multi-mode fibres provide excellent performance with low losses and small dimension, however, they are labour intensive for installation, resulting in high cost and not simple to be deployed in a in-home network [11]. Another solution that has been increasingly studied is the polymer or plastic optical fibres (POFs). POFs are an emerging solution for short reach transmission in term of throughput-cost ratio due largely to their do-it-yourself solution, small bending radius and EMI-free, hence they can be installed in the same ducts next to power cables. Among the different types of POFs, the most popular for indoor communications is the 1-mm core size polymethyl methacrylate (PMMA) step index POF [12], [13]. In this work we use the POF Eska GH4001 that has 1-mm diameter core size and PMMA core material. This POF works in the visible wavelength range (400–700 nm), which enables visual link testing, thus easing the installation. The major drawback for POFs is their relatively low bandwidth-length product, i.e approximately 40 MHz $\times$ 100 m that is caused by the large core of the POF that leads to high intermodal dispersion [13].

One way to overcome this problem is to use spectral efficient modulation formats. The DMT modulation has been investigated and Gbps throughput were reported [14], [15]. DMT is a multiple subcarrier modulation that is a baseband version of the orthogonal frequency division multiplexing (OFDM). In contrast to the traditional OFDM, DMT has a prior knowledge to the channel to maximize throughput by means of power and bit loading [16]. Another simple and cost-effective modulation format that can be used to transmit a baseband signal is the pulse amplitude modulation (PAM). In comparison to DMT, the PAM modulation can be used with more relaxed requirements for bandwidth and transceiver's structure. PAM modulation consists of encoding the messaging information in the amplitude of a series of signal pulses. The on-off keying (OOK) is the simplest PAM format, however it has low spectral efficiency (1 b/s/Hz) [16], [17]. To increase the spectral efficiency, higher order PAM can be used, such as PAM-4, where $\log_2(M)$ bits are transmitted per symbol [16], [18]. In [19] a comparison in transmitting 10 Gbps using OOK and PAM-4 through 300 m POF-only, thus no wireless link, was demonstrated. One major drawback of the DMT is its high peak-to-average power ratio (PAPR). An alternative modulation format that can provide high spectral efficiency with low PAPR and more relaxed requirements on electrical components is the Nyquist-shaped subcarrier modulation (SCM). In [18] the advantages on using Nyquist SCM are presented and a throughput of 112 Gbps over more sophisticated single mode silica fibre in a data center is achieved.

In a typical VLC system, multiple luminaires, which carry the same data (i.e. spatial diversity), are installed per room in order to provide users with a mobility coverage and an alternative path in case of non-line of sight. In addition, users in the line-of-sight served by multiple luminaires can see their received signal becoming better because of increasing received power. This work presents a novel concept for a bidirectional spatial diversity transmission using POF as feeder line to each room ceiling, and the light emitted from the POF-end is used to transmit data, resulting a passive optical front-end (OFE) in-home transmission, thus no dedicated luminaire is needed. We propose a system where the wireless source is composed by a POF-end and a lens placed at a defocused distance in order to extend the coverage area, which consequently increases the number of users and allows mobility, as presented in Fig. 1. In this work we present an extensive analysis on the system performance with different modulation formats for the downlink and uplink. Preliminary results for the downlink were presented in [20]. It is important to highlight that the results were achieved with the use of low power LDs for POF. Taking into account the losses in the POF and splitter, the optical power emitted to the wireless link is considerably below the eye safety limit. Therefore, there is still margin to improve the link budget and, in consequence, increase the link performance. Also, we focus on the use of spatial diversity concept as a form of network

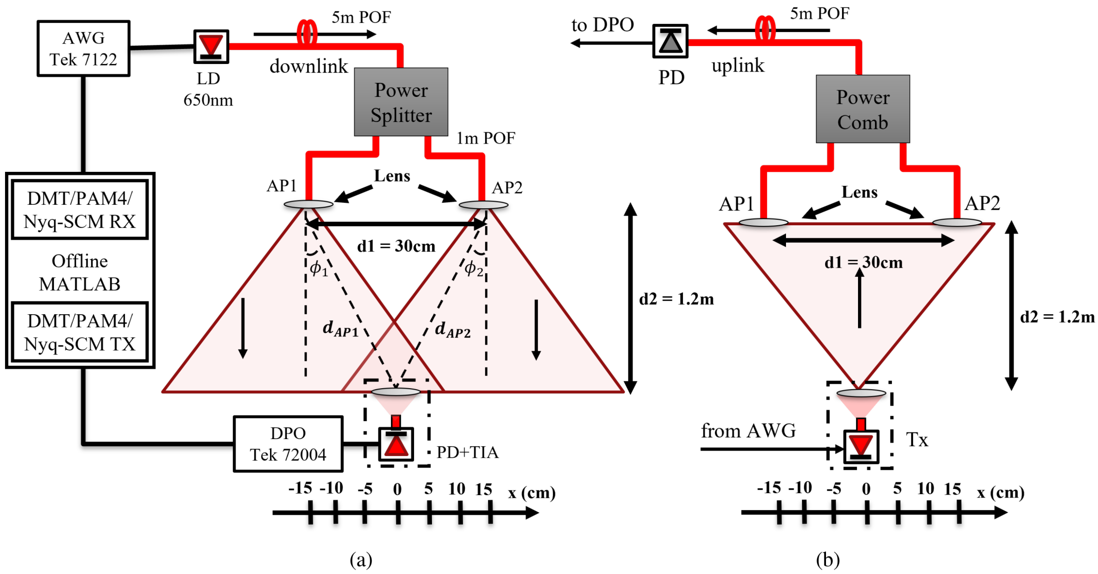

Fig. 2. POF as luminaires: schematic, where the red path refers to the optical link for the downlink (a) and for the uplink (b).

function and not to achieve transmission records. With the use of spatial diversity we can increase coverage areas, ensure inter-cell handovers, and mitigate the effect of non-line of sight. This paper is organized as follow: Section II the concepts for implementing the POF-based wireless system are presented and also. In Section III we elaborate the experimental setup and evaluate the performance for each modulation format and a comparison between all the modulation formats is presented in IV. Finally, in Section V the main conclusions of this paper are presented.

II. POF Concepts for VLC System

In our concept, POFs are used as an analogue fronthaul to interconnect each room to the RG, where last meter connectivities are provided by VLC channel and the user devices transmit/receive the signal to/from POF-ends, as shown in Fig. 1(a). At the ceiling of each room, a lens is placed in front of the POF-end to modify the beam divergence, caused by the POF large numerical aperture, and mark the size of the coverage area.

In our previous work reported in [10], we explored a system comprising the use of optical fibres as feeder line to the room ceilings, using passive OFE for the wireless link, where the light sources are remotely fed, and a lens is placed in front of the POF-end in a focused position. Therefore, small but high capacity wireless cells or multi-Gbps hotspots can be created in a room. In this work we create relatively large wireless cells by employing defocused lenses, which allow users to move between cells. We measure the transmission performance at various position relative to the access points. In Fig. 2(a), (b) the system's diagram for the downlink and uplink can be seen, respectively. For the downlink, the transmitter is comprised of one distributed feedback laser laser and one 2×1 power combiner/splitter. The used LD operates in the wavelength of 658 nm (red light). The LD is directly modulated in the linear region and butt-coupled into the POF. The emitting light from the LD is transmitted through 5 m POF, divided by the power splitter

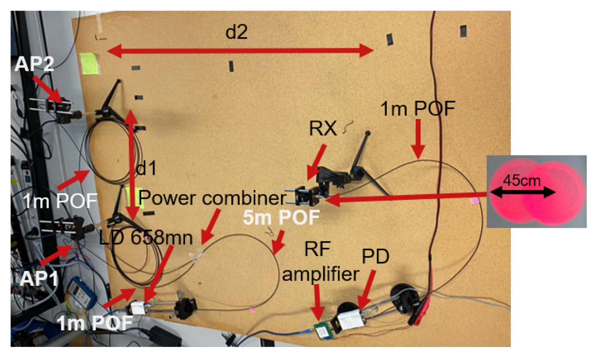

Fig. 3. Experimental setup for the system.

and transmitted through 1 m POF. In front of each POF-end a lens is placed at a defocused distance to create a coverage area of 45 cm diameter, as presented in Fig. 3. If no lens is placed to mark the coverage area, and considering the NA = 0.5 of the PMMA-POF, the light exiting the POF will be launched with a half angle of 30°, resulting in a highly divergent beam. For the uplink, the transmitter is composed by the LD, then the light beam is coupled into a short length POF. In the downlink, the emitting optical power to the wireless link is −6 dBm for AP_1 and −7 dBm for AP_2. For the uplink, the emitting optical power to the wireless link is −4 dBm. For the downlink, in the receiver side the beam is received and coupled into the fibre, and subsequently detected by an optical receiver composed by a SiPD and a transimpedance amplifier (TIA). In the uplink, at the receiver side the signal is received by another lens, coupled into the POF, combined with the power combiner and then received by the optical receiver. The used receiver has a detection bandwidth of 1.2 GHz. The measurements were realised with the lights on, and no noticeable change was observed when switching the lights on/off. Different modulation formats are employed to evaluate the link performance when a user moves from one cell to another: DMT, OOK, PAM-4 and Nyquist-SCM.

III. Experimental Results and Discussion

The schematic of the experimental setup for down- and uplink can be seen in Fig. 2(a), (b), respectively. The distance between the two POF-ends acting as APs transmitters is represented as d_1 and it is set as 30 cm, d_2 represents the distance between the POF and the receiver and it is set as 1.2 m. These distances are chosen largely due to the use of a visible light laser of the class 1 which is safe for all reasonably anticipated conditions of use. The x axis, at the receiver side, represents the position of the user, where the position 0 is equivalent to the position in the middle of the POF-end transmitters AP_1 and AP_2, and the positions -15 and +15, represent the position in front of AP_1 and AP_2, respectively. The performance of the system is characterized by measuring the receiver performance at various x-positions of the receiver, representing the user movement. The branches of the power combiner have different losses, leading to an asymmetric performance. To evaluate the system's performance, transmissions using OOK, PAM-4, DMT and Nyquist SCM formats are realised and their performances are compared and presented in Section IV. In Fig. 8 at Section IV it is possible to observe that the performance of the system is dependent on the position of the receiver. The received power depends on the distance between transmitter and receiver. At position 0, the receiver receives signal from both APs, thus the received power is the sum of the received power from AP_1 and AP_2. Hence, at position 0, better link budget margin is obtained and, consequently, higher SNR and throughput.

A. Discrete Multitone Modulation

For obtaining a high spectral efficiency, DMT divides the passband serial signal into multiple parallel streams and transmits using quadrature amplitude modulation (QAM). The DMT transmitted signal is generated by a pseudo-random binary sequence (PRBS) with 128 subcarriers and is transmitted to estimate the channel. These subcarriers allow the system to achieve its maximum performance with bit error rate (BER) values of around 10^{-3}. By inserting a cyclic prefix, whose length is multiple copies of the data bits, the intersymbol interference (ISI), that may arise from the POF multi-modal dispersion, can be significantly reduced. The DMT signal suffers from high PAPR. A common way to reduce the dynamic range of the DMT signal is by clipping the time-discrete DMT waveform in the digital domain, resulting in a clipped electrical DMT signal $\hat{x}(t)$ after the D/A conversion.

$$\hat{x}(t) = \begin{cases} x(t) \text{ for } |x(t)| \leq A_{\text{clip}} \\ A_{\text{clip}} \text{ for } |x(t)| > A_{\text{clip}} \end{cases} \quad (1)$$

where A_{clip} is the maximum allowed amplitude level and $x(t)$ is the DMT signal without clipping. The modulated signal is now represented by $\hat{x}(t)$ and its clipping-limited crest factor μ is defined by (2) depending on the amount of clipping:

$$\mu = \frac{A_{\text{clip}}}{\sqrt{\langle x^2(t) \rangle}} \quad (2)$$

where $\langle x^2(t) \rangle$ represents the mean power of the DMT time signal $x(t)$ without clipping. In this work the clipping of the DMT signal is set to 9 dB. The performance of the system is optimized by means of bit and power loading with the use of a Chow's rate adaptive bit-loading algorithm.

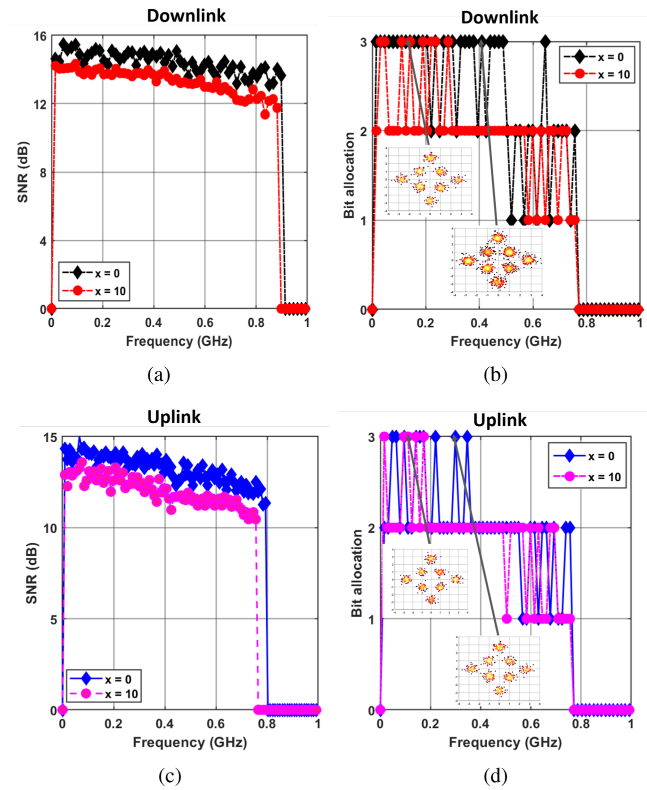

Fig. 4. Link performance for position 0 and 10 versus subcarrier frequencies: SNR (a), bit allocation (b) for the dowlink, SNR (c), and bit allocation (d) for the uplink.

The 128-subcarrier PRBS DMT signal is generated using an arbitrary waveform generator (AWG) that is used as a digital-to-analog converter (DAC). In the receiver, the signal is received by a digital phosphor oscilloscope (DPO), that works as a analog-to-digital converter (ADC), and sampled by 50 GSa/s. Afterwards the signal processing is realised offline and signal-to-noise ratio (SNR), throughput and BER counting are performed for different receiver positions.

In Fig. 4 the received SNR and bit allocation for each receiver position in the downlink and uplink are presented. In addition, in the insets of Fig. 4, the constellations for the receiver position 0, where the highest received power is obtained, and receiver position 10, where the lowest received power is obtained, for downlink and uplink, are respectively depicted. A clear separation between the constellation of the 8-QAM levels can be seen, indicating an excellent transmission performance. The presented constellation is obtained for the subcarriers below 400 MHz. For higher frequencies, a clear separation is still noticed, however, with lower QAM levels.

In Fig. 9(a), (b), the blue curves represent the DMT throughput for each receiver position for the downlink and uplink, respectively. In the overlapping area, where the receiver is obtaining the higher signal strength, 3.3 Gbps throughput is achieved for the downlink, and 2.6 Gbps for the uplink. When moving to another cell, position 10, where the receiver has the lowest signal strength, 1.8 Gbps throughput for the downlink and 1.7 Gbps for the uplink is achieved.

In Fig. 10, the reference level of the transmission is presented for various optical input power. The reference level throughput is defined as the POF-only throughput measured before the wireless channel, thus at the output of AP_1 or AP_2. From the reference throughput we can measure the penalty due to the wireless channel. For example, for position 0 the received power in Fig. 9(a), (b) is -13.2 dBm (downlink, 3.3 Gbps blue curve) and -14.6 dBm (uplink, 2.6 Gbps blue curve). If we use a POF-only link with the same optical transceiver, these received powers, according to Fig. 10 (blue curve), correspond to the throughputs of approximately 3.8 and 3.4 Gbps, respectively. The difference in throughput gives the penalty. Thus, for position 0 the penalty due to wireless link is $3.8–3.3 = 0.5$ Gbps and $3.4–2.6 = 0.8$ Gbps for down- and uplink, respectively. If we measure penalties using the same method for all positions, then we observe penalty levels of less than 0.8 Gbps for down- and uplink. These penalties are quite significant given the obtained down- and uplink throughput, hence design and fabrication of optical front-ends to capture as much light as possible is important for optimizing wireless links. This finding will be addressed in our future studies.

B. Pulse Amplitude Modulation

In comparison to DMT, a simple and cost-effective modulation format to transmit a baseband signal is PAM. It can be used with more relaxed requirements for bandwidth and has simple transmitter and receiver structures. PAM consists of encoding the messaging information in the amplitude of a series of signal pulses. OOK or PAM-2 is the simplest optical pulse modulation format and is primarily used for link conditions that have low SNRs. In the OOK modulation, a binary data is transmitted and encoded into the optical signal's amplitude. In this modulation two amplitude levels are used to carry the data (0 and 1), where each symbol represents a single bit and therefore, OOK has a spectral efficiency equal to 1 b/s/Hz. If an optical wireless link has moderate-to-high SNRs, the link spectral efficiency can be improved by transmitting multiple bits per symbol. For the PAM-M, $\log_2(M)$ bits are encoded per symbol and the symbol alphabet is given by $[\pm 1, \pm M]$, thus the spectral efficiency improves, but at a cost of a higher SNR requirement. The 2-bit encoded in the PAM-4 format results in a four-level signal. A Gray-coded mapping from bits to symbols is used to reduce the number of errors in the transmission. Similar to the DMT experiments, the OOK and PAM-4 signals were generated using the same DAC at the transmitter and ADC at the receiver. We used the same offline processing to evaluate the wireless link performance for different receiver positions. In Fig. 5, the eye diagrams for downlink and uplink using OOK and PAM-4 with the receiver in position 0 and 10 are presented. An equal and clear separation can be seen among the levels of the eye diagram, indicating an excellent performance for both OOK and PAM-4.

In Fig. 9(a), the downlink throughput for each receiver position is presented, where the pink curve represents the OOK throughput and the red curve the PAM-4 throughput. For the downlink, a maximum throughput of 1.6 Gbps and 2.6 Gbps are achieved for the OOK and PAM-4 modulation in the overlapping area, respectively. At the position 10, when the receiver is in another cell, with the lowest signal strength, a throughput of 0.7 Gbps and 1.3 Gbps are achieved for the OOK and PAM-4 modulation for the downlink, respectively. In Fig. 9(d), the throughputs for the uplink for each receiver position is presented, where the pink line represents the OOK throughput and the red line the PAM-4 throughput. A maximum throughput of 1.4 Gbps and 2.1 Gbps are achieved, for the OOK and PAM-4 modulation at position 0, respectively. When the receiver has the lowest signal strength, at position 10, a throughput of 0.6 Gbps and 1.3 Gbps are achieved for the OOK and PAM-4 modulation, respectively.

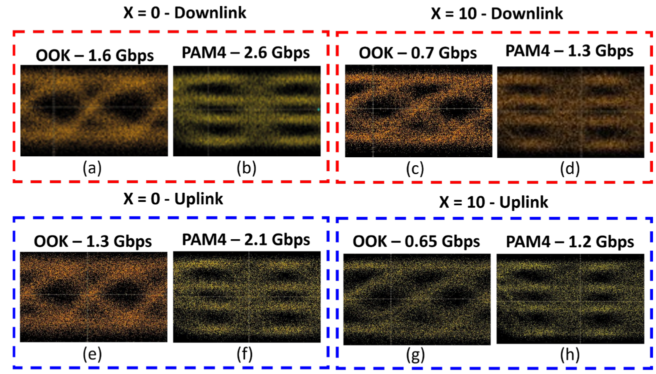

Fig. 5. Down- and uplink performance showing eye diagrams for OOK and PAM-4 and for position 0 and 10. Downlink: (a) OOK and (b) PAM-4 for position 0; and (c) OOK and (d) PAM-4 for position 10. Uplink: (e) OOK and (f) PAM-4 for position 0 and (g) OOK and (h) PAM-4 for position 10.

C. Nyquist-Scm Qam

The DMT modulation offers high spectral efficiency, but suffers from a high PAPR of the signal. The high PAPR leads to severe requirements on electrical components, and consequently limiting the system's performance. One alternative modulation format that can be used to increase spectral efficiency with low PAPR is the Nyquist-SCM.

The Nyquist-SCM modulation uses quadrature amplitude modulation (QAM) with an electrical RF subcarrier, that is intensity modulated on the optical carrier. The baseband signal has its bandwidth reduced by means of a Nyquist pulse shaping modulated onto a single subcarrier and then converted to an optical signal. To reduce the electro-optical bandwidth requirement, the subcarrier frequency (f_{SC}) needs to remain as low as possible. In the single-cycle SCM approach, the f_{SC} can be set equal to the symbol rate f_{symb} to avoid aliasing. In this way the required overall optical bandwidth is the double of the symbol rate. In order to reduce the bandwidth requirement, a Nyquist filtering is applied, and ideally, the bandwidth can be restricted to $f_{symb}/2$, enabling the SCM signal without aliasing even with the subcarrier frequency defined as half of the symbol rate. This approach is known as half-cycle SCM. The generation of an ideal Nyquist-shaped signal would use a roll-off factor equals

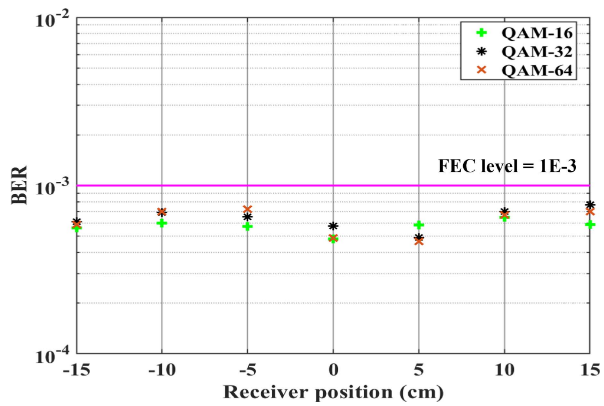

Fig. 6. Estimated BER for each receiver position obtained from the measured EVM values of the system.

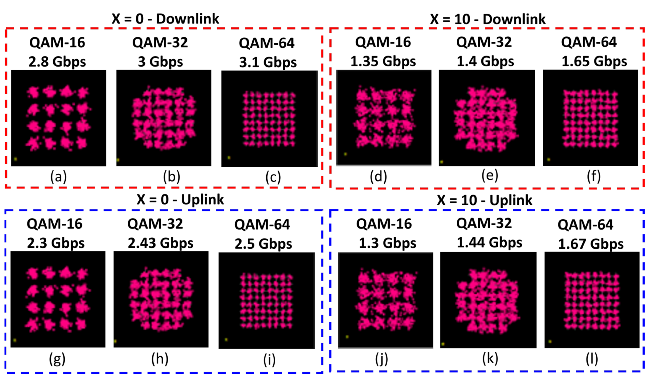

Fig. 7. Nyquist SCM constellation of uplink for receiver position 0 with 16-QAM (a), 32-QAM (b), 64-QAM (c) and Nyquist SCM constellation for receiver position 10 with 16-QAM (d), 32-QAM (e) and 64-QAM (f).

to 0, however this raises a high challenge for the digital filter implementation.

The Nyquist SCM signals are generated by means of the RF Xpress software in the AWG, with a roll-off factor of 1%. In the receiver, the signal is then received by a DPO and sampled by 50 GSa/s. In Fig. 9(a) the throughput for each receiver position is presented and the green, black and brown line represent, respectively, the throughput results for 16-QAM, 32-QAM and 64-QAM. Three levels of M-QAM signal were generated and their constellations are presented in Fig. 7. A clear and equal separation between the constellation levels can be seen, which indicates an excellent performance. For the previous results we fixed the BER below the FEC level ($< 10^{-3}$) and obtained the highest throughput within the fixed BER. For the Nyquist SCM measurements, the used software provide us with the error vector magnitude (EVM) value, instead of BER. However, with the use of (3) we can calculate the BER value from the EVM results [21]. In this way, we can guarantee that our BER in all the positions is below the FEC threshold of error-free operation, and that we achieved the highest throughput for a BER value of around 10^{-3}.

$$\mathrm{BER} \approx \frac{2\left(1-\frac{1}{L}\right)}{\log_2 L} Q\left[\sqrt{\left(\frac{3\cdot\log_2 L}{L^2-1}\right)\left(\frac{2}{\mathrm{EVM}_{\mathrm{rms}}^2\cdot\log_2 M}\right)}\right] \tag{3}$$

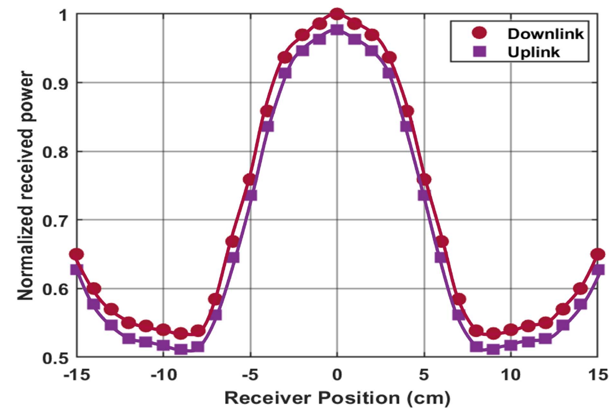

Fig. 8. Theoretical normalized received power per receiver position.

where L represents the number of levels in each dimension of the M-ary modulation system, and $Q(.)$ is the Gaussian complementary error function. In the case of 16/32/64-QAM, $L = 4/5/6$ and $M = 16/32/64$. In Fig. 6, we present the BER values for each receiver position calculated using (3). It can be seen that the BER values for all the receiver positions are below the FEC level.

IV. Performance Comparison Between DMT, PAM-4, OOK and Nyquist SCM

In the previous section, the results of the transmission using three types of modulation format (DMT, PAM and Nyquist SCM) have been analyzed. In this section their performance will be compared.

In Fig. 9(a), (b) a comparison of the throughput per receiver position is presented. At position 0, where the receiver is in the middle of the overlapping area, the maximum throughput is obtained. The light launched from the POF is emitted in an axially symmetric pattern, thus the power at the receiver P_{RX} as a function of the position is defined as:

$$P_{RX} = \frac{P_{TX} R_\sigma(\phi)}{d^2} \cdot A_{\mathrm{eff}}(\psi) \tag{4}$$

where P_{TX} is the wireless transmitted power, A_{eff} is the effective area of the receiver, d is the distance between transmitter and receiver and $R_\sigma(\phi)$ is the radiant intensity, as seen in Fig. 2(a). For a Lambertian model transmitter, the radiant intensity is given by:

$$R_\sigma(\phi) = \left[\frac{(m+1)}{2\pi}\right]\cos^m(\phi) \tag{5}$$

where m is related to the transmitter semi-angle at half-power, $m = -\frac{\ln 2}{\ln(\cos(\phi_{1/2}))}$. For a Lambertian transmitter $\phi_{1/2} = 60°$, thus $m = 1$. Replacing (6) and (5) in (4), P_{RX} is written as:

$$P_{RX} = \frac{P_{TX}\cos(\phi)}{d^2} \cdot A_{\mathrm{eff}}(\psi) \tag{6}$$

From (6) the wireless received power can be estimated. The performance of the system is influenced by the received power. The highest powers have consequently highest SNRs, thus better

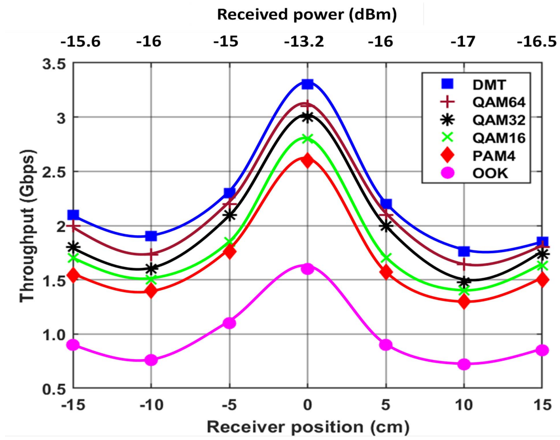

(a)

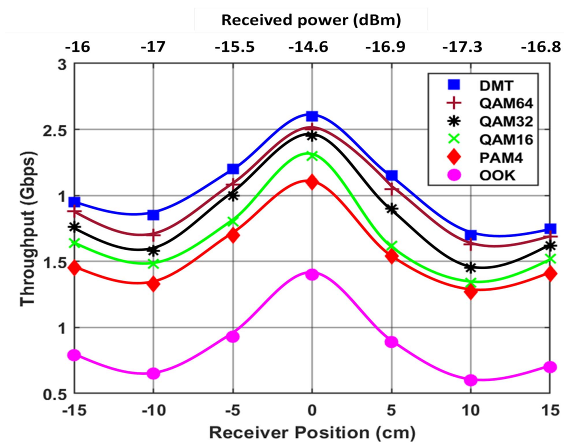

(b)

Fig. 9. Link performance comparison of 1.2 m VLC transmission for the downlink (a) and uplink (b) for different receiver positions and modulation formats.

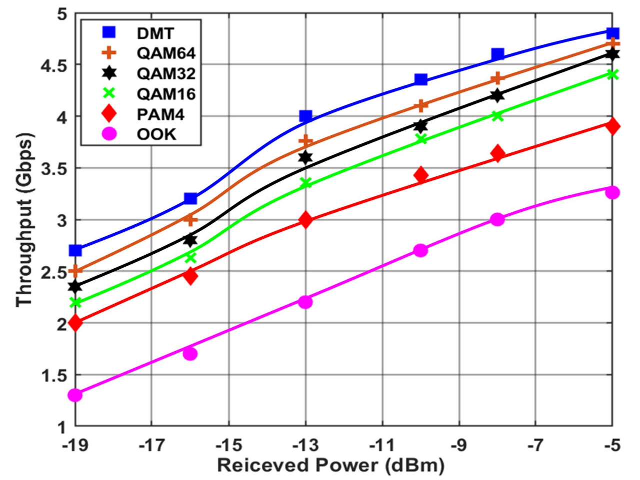

Fig. 10. Reference level throughput measured at the POF output, before the wireless link.

performance. Fig. 8 presents the estimation of the wireless received power versus the receiver positions using (6). Comparing Figs. 8 and 9 we can notice that the shape of the curve is similar and the positions for the maximum and minimum link throughput are well described, showing that the experimental results are consistent with our prediction.

In Fig. 9(a) it can be noticed that the maximum throughput is obtained at position 0, that represents the receiver positioned in the middle of the overlapping area. At this position, the receiver is obtaining signal contributions from both APs. From (6) it can be seen that in the overlapping area, the received power will be the sum of the power received from AP_1 and AP_2 leading to an increase in SNR of the signal and, consequently, increasing the throughput. When the user is placed at position +15, it is only receiving signal from AP_2, however, the distance between AP_2 and the user at position +15 is smaller than when the user is placed at position +10. As seen from (6), the received power is associated with the distance between AP and receiver, thus for this reason, the received power in +15 is larger than in +10, and consequently providing a better performance. The same analysis can be realized when the user moves towards position −15. When moving from one cell to another, the user can experience a throughput variation of 1.4−1.5 Gbps. The DMT modulation transmission achieves 3.3 Gbps, providing a better performance compared to the other modulations. However, 64-QAM Nyquist-SCM offers a performance similar to DMT, achieving 3.1 Gbps and from practical perspectives it can be beneficial for the RF circuitry of light sources because Nyquist-SCM does not produce high PAPR values, resulting in the maximum utilization (thus no use of clipping) of the modulating signals. The use of PAM-4 with lower throughput, 2.7 Gbps, can also be beneficial because it allows us to use much simpler optical transmitters and receivers when compared to DMT and Nyquist-SCM, resulting in lower cost and power consumption, which are important features for inhome wireless terminals. The asymmetric performance of AP_1 and AP_2 presented in Fig. 9(a) is related to the asymmetric splitting ratio of each branch of the power splitter.

In Fig. 9(b), the performance for the uplink is presented. From (6) it can be shown that the received power in position 0 will be the sum of the received power in AP_1 and AP_2, thus in position 0 the highest power is obtained and, consequently, the highest throughput. The DMT modulation offers the highest throughput of 2.6 Gbps, providing the best performance when compared to the other modulation formats. The use of a power combiner and a single light source from the mobile user has incurred less link budget than the downlink, resulting in a slightly lower throughput performance for the uplink.

In Fig. 10, the performance of the reference level from our system is presented. The reference level is defined as the point at the POF-end and prior to the wireless channel, thus, exactly in the output of the AP. Analysing Figs. 9(a) and 10 we can conclude that the penalty in the downlink throughput caused by the power variation in the wireless channel due to the user position is less than 1 Gbps.

Previous results showed link performance for the case where both APs are in line of sight with the receiver, hence the receiver gets optical signals from both APs. If one of APs is blocked by an obstacle, then the power in the receiver drops and therefore SNR values also drop. The overall throughput will be less than in the case of line of sight, as shown in Table I.

TABLE I
LINK PERFORMANCE WITH ONE OF APS IN NON-LINE OF SIGHT WITH THE RECEIVER AT POSITION 0

	DMT (Gbps)	OOK (Gbps)	PAM-4 (Gbps)	16-QAM (Gbps)	32-QAM (Gbps)	64-QAM (Gbps)
Only AP_1	1.5	0.8	1.1	1.25	1.35	1.4
Only AP_2	1.4	0.65	1	1.2	1.25	1.36

V. CONCLUSION

Inhome communication networks should topologically be very simple and employ very low-cost components due to no cost-sharing mechanism when installing and operating these networks. Here, we presented a novel indoor communication system using POFs as feeder line to the room ceilings, using the light emitted by the POF-end to transmit data, resulting in passive OFEs and, consequently, no dedicated luminaires are needed. This approach allows to accommodate user movements and non-line of sight transmission with spatial diversity. The presented experimental results comprise the system's performance for downlink and uplink. To characterize the system's performance, transmissions using different modulation formats (PAM, DMT and Nyquist SCM) were realised. For the downlink, the DMT transmission provided the best performance, achieving 3.3 Gbps throughput. However, 64-QAM Nyquist-SCM can also provide high performance, achieving 3.1 Gbps. Simple PAM-4 can also be used, even with lower throughput of 2.6 Gbps. For the uplink the best performance is also achieved using DMT, providing 2.6 Gbps, while for the 64-QAM Nyquist-SCM 2.5 Gbps is achieved, and 2.1 Gbps for PAM-4.

The use of 64-QAM Nyquist SCM can offer high performance with the benefit of allowing more relaxed requirements on electrical components, due to its low PAPR. The use of PAM-4 can be beneficial once it can simplify the baseband transceiver's architecture, which results in lower power consumption and cost. The user's movement from one cell to another will have an impact in the link performance, but with the proposed solution, a throughput >1 Gbps can be guaranteed.

Further works will include the implementation of wavelength division multiplexing to improve coverage area and throughput via spatial multiplexing, real-time transmission employing commercial chip-sets, and also designing of optical front-ends for increasing captured light for a higher link budget. We believe the proposed concept of using a passive OFE with POF as feeder line, without employing any dedicated luminaire, is a potential low-cost technique for high capacity indoor wireless communication systems.

REFERENCES

[1] S. M. Kouhini et al., "Distributed mimo experiment using LiFi over plastic optical fiber," in *Proc. IEEE Globecom Workshops (GC Wkshps)*, 2020, pp. 1–6.

[2] T. Koonen, K. A. Mekonnen, F. Huijskens, N. Pham, Z. Cao, and E. Tangdiongga, "Fully passive user localization for beam-steered high-capacity optical wireless communication system," *J. Lightw. Technol.*, vol. 38, no. 10, pp. 2842–2848, 2020.

[3] C.-Y. Li et al., "White-lighting and WDM-VLC system using transmission gratings and an engineered diffuser," *Opt. Lett.*, vol. 45, no. 22, pp. 6206–6209, Nov. 2020.

[4] L.-Y. Wei, C.-W. Hsu, C.-W. Chow, and C.-H. Yeh, "40-Gbit/s visible light communication using polarization- multiplexed R/G/B laser diodes with 2-M free-space transmission," in *Proc. Opt. Fiber Comnmu. Conf. Exhib.*, 2019, pp. 1–3.

[5] T.-C. Wu, Y.-C. Chi, H.-Y. Wang, C.-T. Tsai, Y.-F. Huang, and G.-R. Lin, "Tricolor R/G/B laser diode based eye-safe white lighting communication beyond 8 Gbit/s," *Sci. Rep.*, vol. 7, no. 1, Jan. 2017, Art. no. 11.

[6] F. Zafar, M. Bakaul, and R. Parthiban, "Laser-diode-based visible light communication: Toward gigabit class communication," *IEEE Commun. Mag.*, vol. 55, no. 2, pp. 144–151, Feb. 2017.

[7] Y.-H. Chang et al., "4.343-Gbps green semipolar (20-21) μ-led for high speed visible light communication," *IEEE Photon. J.*, vol. 13, no. 4, pp. 1–4, 2021.

[8] H. Haas et al., "Introduction to indoor networking concepts and challenges in LiFi," *J. Opt. Commun. Netw.*, vol. 12, no. 2, pp. A190–A203, 2020.

[9] K. L. Bober et al., "Distributed multiuser mimo for LiFi in industrial wireless applications," *J. Lightw. Technol.*, vol. 39, no. 11, pp. 3420–3433, 2021.

[10] C. R. B. Corrča, F. M. Huijskens, E. Tangdiongga, and A. M. J. Koonen, "Luminaire-free gigabits per second LiFi transmission employing WDM-over-POF," in *Proc. Eur. Conf. Opt. Commun.*, 2020, pp. 1–4.

[11] I. Mollers et al., "Plastic optical fiber technology for reliable home networking: Overview and results of the EU project POF-ALL," *IEEE Commun. Mag.*, vol. 47, no. 8, pp. 58–68, Aug. 2009.

[12] A. M. J. Koonen and E. Tangdiongga, "Photonic home area networks," *J. Lightw. Technol.*, vol. 32, no. 4, pp. 591–604, 2014.

[13] O. Ziemann, O. Krauser, P. Zamzow, and W. Daum, *POF Handbook: Optical Short Range Transmission Systems*. Berlin, Germany: Springer, 2008.

[14] S. C. J. Lee et al., "Discrete multitone modulation for maximizing transmission rate in step-index plastic optical fibers," *J. Lightw. Technol.*, vol. 27, no. 11, pp. 1503–1513, 2009.

[15] M. Jončić, R. Kruglov, M. Haupt, R. Caspary, J. Vinogradov, and U. H. P. Fischer, "Four-channel WDM transmission over 50-m SI-POF at 14.77 Gb/s using DMT modulation," *IEEE Photon. Technol. Lett.*, vol. 26, no. 13, pp. 1328–1331, Jul. 2014.

[16] S. Randel, F. Breyer, S. C. J. Lee, and J. W. Walewski, "Advanced modulation schemes for short-range optical communications," *IEEE J. Sel. Topics Quantum Electron.*, vol. 16, no. 5, pp. 1280–1289, Sep./Oct. 2010.

[17] P. J. Winzer and R.-J. Essiambre, "Advanced modulation formats for high-capacity optical transport networks," *J. Lightw. Technol.*, vol. 24, no. 12, pp. 4711–4728, 2006.

[18] P. Bakopoulos, S. Dris, N. Argyris, C. Spatharakis, and H. Avramopoulos, "112 Gb/s sub-cycle 16-QAM Nyquist-SCM for intra-datacenter connectivity," in *Int. Soc. Opti. Photon.*, 2016, pp. 56–64. [Online]. Available: https://doi.org/10.1117/12.2211639

[19] F. Breyer, S. J. Lee, S. Randel, and N. Hanik, "Comparison of OOK- and PAM-4 modulation for 10 Gbit/s transmission over up to 300 m polymer optical fiber," in *Proc. OFC/NFOEC 2008-2008 Conf. Opt. Fiber Commun./Nat. Fiber Optic Engineers Conf.*, 2008, pp. 1–3.

[20] C. R. B. Corrča, E. Tangdiongga, and A. M. J. Koonen, "Spatial diversity performance of DMT, PAM4 gigabits per second transmission using POF as luminaires," in *Proc. Opt. Fiber Commun. Conf. Exhib. (OFC)*, 2021, pp. 1–3.

[21] A. Trinidad, N. Tessema, X. Zhang, Z. Cao, E. Tangdiongga, and A. Koonen, "Evaluation of PAM-4, DMT, and Nyquist-SCM for multi-Gbps transmission on bandwidth-limited ORR-based beamformer," in *Proc. Eur. Conf. Opt. Commun.*, 2018, pp. 1–3.

Carina Barbio (Student Member, IEEE) received the B.Eng. degree in telecommunication engineering from Federal Fluminense University (UFF), Rio de Janeiro - Brazil, in 2015, and the M.Sc. degree in electrical and telecommunication engineering from Federal Fluminense University (UFF), Rio de Janeiro - Brazil in 2018. She is currently working toward the Ph.D. degree with the Eindhoven University of Technology, The Netherlands. Her research interests include optical wireless communication, visible light communication, plastic optical fibre as feeder line, and passive optical front-ends for VLC systems.

Ketemaw Addis Mekonnen (Member, IEEE) received the B.Sc. degree in electrical engineering from Mekelle University, Mek'ele, Ethiopia, in 2007, the double M.Sc. degree with the Erasmus Mundus Master on Photonic Networks Engineering Program from Scuola Superiore Sant'Anna, Pisa, Italy, and Aston University, Birmingham, U.K., in 2013, and the Ph.D. degree from the Eindhoven University of Technology, The Netherlands, in 2018. His research interests include dynamic optical routing, radio over fiber, signal processing, and optical wireless communication.

Frans Huijskens received the B.Eng. degree in applied physics from the Technical College of Dordrecht, The Netherlands, in 1979. From 1981 to 1984, he was an Electronic Test Engineer with Siemens Gammasonics. In 1985, he joined the Electro-Optical Communications Group of Eindhoven University of Technology, Eindhoven, The Netherlands. He worked on passive fiber components, phase- and polarization-diversity coherent systems, on demonstrator setups of optical crossconnecting, optical packet switching, few-mode fiber transmission, and on packaging of optical integrated devices. His current research focuses on demonstrator setups of optical wireless communication.

Ton Koonen (Fellow, IEEE) is currently a Professor emeritus since 2021 with the Eindhoven University of Technology, The Netherlands. From 2001, he was a Full Professor and in 2004–2021 chaired the Electro-Optical Communication System Group. In 2016–2019, he was the Scientific Director of Institute of Photonic Integration, which is now named Eindhoven Hendrik Casimir Institute. Before 2001, he worked for more than 20 years in applied research in industry, Bell Labs-Lucent Technologies being one of them. Ton is a Bell Labs Fellow (1998, first one in Europe), IEEE Fellow in 2007, OSA Fellow in 2013, Distinguished Guest Professor of Hunan University, Changsha, China in 2014, and High-level Visiting Scientist with the Beijing University of Posts and Telecommunications, Beijing, China (111 Program, 2018–2023). In 2012, he was the recipient of a prestigious Advanced Investigator Grant of the European Research Council on optical wireless communication, followed by a Proof-of-Concept Grant in 2018. His research interests incldue broadband (optical) communication networks and techniques, currently in particular optical in-building networks (including optical wireless communication techniques, radio-over-fiber techniques, and high-capacity plastic optical fiber techniques), optical access networks, and spatial division multiplexed systems.

Eduward Tangdiongga (Member, IEEE) received the M.Sc. and Ph.D. degrees from the Eindhoven University of Technology, Eindhoven, The Netherlands, in 1994 and 2001, respectively. In 2001, he joined COBRA Research Institute, currently named Eindhoven Hendrik Casimir Institute, working on ultrafast optical signal processing using special optical fibres and optical semiconductor devices. In 2016, he became an Associate Professor on advanced optical access and local area networks. His research interests include passive optical networks, radio over (single mode-, multimode-, and plastic) fiber, intelligent antenna systems, and free-space optics/optical wireless communication.